Hysteresis loop areas in kinetic Ising models: Effects of the switching mechanism

S.W. Sides,^{*†‡} P.A. Rikvold,^{*†‡} and M.A. Novotny [†]*

*Center for Materials Research and Technology and Department of Physics, and [†]Supercomputer Computations Research Institute,

Florida State University, Tallahassee, Florida 32306-4130

[‡]Colorado Center for Chaos and Complexity, University of Colorado, Boulder, Colorado

80309-0216

*Department of Electrical Engineering, FAMU-FSU College of Engineering,

Pottsdamer Street, Tallahassee, Florida 32310-6046

(March 24, 2022)

Abstract

Experiments on ferromagnetic thin films have measured the dependence of the hysteresis loop area on the amplitude and frequency of the external field, $A=A(H_0,\omega)$, and approximate agreement with numerical simulations of Ising models has been reported. Here we present numerical and theoretical calculations of A in the low-frequency regime for two values of H_0 , which bracket a temperature and system-size dependent crossover field. Our previous Monte Carlo studies have shown that the hysteretic response of the kinetic Ising model is qualitatively different for amplitudes above and below this crossover field. Using droplet theory, we derive analytic expressions for the low-frequency asymptotic behavior of the hysteresis loop area. In both field regimes, the loop area exhibits an extremely slow approach to an asymptotic, logarithmic frequency dependence of the form $A \propto -[\ln(H_0\omega)]^{-1}$. Our results are relevant to the interpretation of data from experiments and simulations, on the basis of which power-law exponents for the hysteresis-loop area have been reported.

PACS number(s):64.60.Qb, 75.60.Ej, 75.10.Hk, 64.60.My

Typeset using $\text{REVT}_{\text{E}}X$

When a ferromagnet is subject to an oscillating external field, $H(t)=H_0 \sin \omega t$, the timedependent magnetization, m(t), typically lags behind the field. The area of the resulting hysteresis loop, $A=-\oint m(H) dH$, equals the energy dissipated per period. It is therefore frequently measured in studies of periodically driven magnetic systems. Recent experiments on ultrathin ferromagnetic films,^{1,2} as well as numerical simulations of two-dimensional Ising models,³⁻⁶ have been interpreted in terms of a low-frequency power law, $A \propto H_0^a \omega^b$, with a range of exponent values having been reported.⁴⁻⁶ This interpretation is not fully consistent with the fluctuation-free mean-field result,^{7,8} $A = A_0 + \text{const}[\omega^2(H_0^2 - H_{sp}^2)]^{1/3}$ with positive constants A_0 and H_{sp} , which has been successfully applied to analyze experiments on ultrathin films of Co on Cu(001).⁹ Nor does the single power-law dependence agree with the logarithmic dependence expected if thermally activated nucleation is the rate-determining process.¹⁰⁻¹² Here we present analytical and numerical results that indicate a resolution of this puzzling situation.

Theoretical arguments and numerical simulations reveal parameter regimes in which, following instantaneous field reversal, a uniaxial single-domain ferromagnet switches to the stable magnetization direction via two distinct mechanisms. This magnetization reversal occurs either by nucleation of a *single* critical droplet of the stable phase [the single-droplet (SD) regime] or by simultaneous nucleation and growth of *many* critical droplets [the multidroplet (MD) regime].^{12–14} The SD (MD) regime corresponds to weaker (stronger) fields and/or smaller (larger) systems. In this extension of our previous studies of hysteresis,¹⁵ we present analytical and Monte Carlo results for the hysteresis-loop area for a kinetic Ising model at low frequencies; both in the SD regime and in the MD regime. The derivations are based on time-dependent extensions of classical homogeneous nucleation theory and "Avrami's law" for the decay of a metastable phase.¹⁶ For both decay mechanisms we show how an extremely slow approach of A to an asymptotic logarithmic dependence on $H_0\omega$ as $\omega \to 0$ gives "effective exponents" which superficially appear to describe a power law, even for data extending over several decades in frequency.

The model used here is a kinetic, nearest-neighbor Ising ferromagnet on a square lattice with Hamiltonian $\mathcal{H}=-J\sum_{\langle ij\rangle}s_is_j-H(t)\sum_i s_i$ and periodic boundary conditions. Here $s_i=\pm 1$ are the local spin variables, $\sum_{\langle ij\rangle}$ runs over all nearest-neighbor pairs, and \sum_i runs over all $N=L^2$ lattice sites. The ferromagnetic exchange coupling is J > 0, and H(t) is a time-dependent external field. The dynamic is the Glauber single-spin-flip algorithm, with updates at randomly chosen sites. It is defined by the spin-flip probability $W(s_i \to -s_i)=$ $\exp(-\beta\Delta E_i)/(1+\exp(-\beta\Delta E_i))$, where ΔE_i is the change in the energy of the system if the spin flip is accepted, and $\beta^{-1} = k_{\rm B}T$ is the temperature in energy units. Time is given in units of Monte Carlo steps per spin (MCSS). The average lifetime, $\langle \tau(|H|) \rangle$, of the unfavorably magnetized phase in a *static* field of magnitude |H| is defined as the average time it takes the magnetization to reach zero, following instantaneous field reversal. The frequency, ω , of the applied sinusoidal field, is chosen by specifying the ratio $R=(2\pi/\omega)/\langle \tau(H_o) \rangle$.

We initially prepare a system of size L=64 at $T=0.8T_c$ with all spins down, i.e. m(0)=-1. Then the sinusoidal field $H(t)=H_0 \sin \omega t$ is applied, and m(t) is recorded for a fixed number of MCSS, n_{max} . For the simulations in the SD regime, the field amplitude is $H_0=0.1J$ (which gives $\langle \tau \rangle = 2058$ MCSS) with $n_{\text{max}}=16.9 \times 10^6$ MCSS. For the MD regime, the amplitude is $H_0=0.3J$ (which gives $\langle \tau \rangle = 75$ MCSS) with $n_{\text{max}}=5.9 \times 10^5$ MCSS. For the values of L and T used here, the crossover field (called the Dynamic Spinodal¹⁴ (DSP)) between these two regimes is $H_{\text{DSP}} \approx 0.11 J$. For large systems H_{DSP} vanishes slowly with L as $H_{\text{DSP}}(L) \sim (\ln L)^{-1/(d-1)}$. Figure 1 shows representative hysteresis loops from simulations in both the SD and MD regimes. The large relative fluctuations in the loop area in Fig. 1(a) indicate the stochastic nature of the switching mechanism in the SD regime.¹⁷ The relative fluctuations in the loop area are smaller in the MD regime (Fig. 1(b)). The stochastic nature of magnetization reversal in the SD regime allows one to treat the switching as a variable-rate Poisson process. For low frequencies, this variable switching rate is the system volume times the nucleation rate obtained from classical droplet theory,

$$L^{d}I(H(t),T) \propto L^{d}|H(t)|^{K} \exp\left[-\frac{\Xi_{0}(T)}{|H(t)|^{d-1}}\right],$$
(1)

where d is the spatial dimension of the system, and K and $\Xi_0(T)$ are known from theory and simulations.^{13,14} The quantity $\Xi_0(T)$ is the field-independent part of the free-energy cost of a critical droplet, divided by $k_{\rm B}T$. The time dependence of the nucleation rate enters solely through H(t). Using Eq. (1) one can derive an expression for the cumulative probability that a switch has taken place by time t, F(t).¹⁷ The median switching time, $t_{\rm s}$, is given by $F(t_{\rm s})=1/2$. To obtain an analytic result we use the low-frequency approximation $H(t) \approx H_0 \omega t$. Then the median switching field, $H_{\rm s}=H_0 \omega t_{\rm s}$, is given by the solution of the equation,

$$\ln 2 = \rho_0 \frac{e^{\frac{\Xi_0(T)}{H_0^{d-1}}} \Xi_0^{\frac{K+1}{d-1}}}{H_0^{K+1}(d-1)\omega} \Gamma\left(1 - \frac{K+d}{d-1}, \frac{\Xi_0}{H_s^{d-1}}\right),\tag{2}$$

where $\Gamma(a, x)$ is the incomplete gamma function, and ρ_0 is the switching rate in a static field of magnitude H_0 , which has been measured in field-reversal simulations.¹⁷

Due to the square shape of the hysteresis loop in both regimes, the loop area is given by $\langle A \rangle / 4H_0 \approx m_{eq}H_s(\omega)/H_0$, where m_{eq} is the spontaneous zero-field magnetization. Figure 2 is a log-log plot of the hysteresis-loop area versus the frequency, 1/R, in the SD regime. The solid curve is calculated by numerical solution of Eq. (2) with d=2, K=3, $\Xi_0=0.506192J$, and $\rho_0=6.62\times10^{-4}\mathrm{MCSS^{-1}}$. Hence, this calculation involves no adjustable parameters. The solid dots are data from MC simulations. Each of the two dashed lines is obtained from a linear least-squares fit to the numerical solution for the loop area over nearly four decades in frequency. The effective exponents obtained from this fitting procedure appear valid over a frequency range that would be considered large from the viewpoint of experiments or even simulations. Over a very large frequency range however, the effective exponent depends on the frequency range in which data are analyzed. Expanding $\Gamma(a, x)$ in Eq. (2) for large values of $x=\Xi_0/H_s^{d-1}$ gives the asymptotic low-frequency result $\langle A \rangle_{\rm SD} \propto -[\ln(H_0\omega)]^{-1/(d-1)}$.

The details of the theoretical derivation of the loop area in the MD regime are different than in the SD regime. However, two basic features are the same: the form of the timedependent nucleation rate, I(H(t), T) from Eq. (1), and the linear approximation for the field used to obtain asymptotic analytic results for very low frequencies. Figure 3 is a log-log plot of the hysteresis-loop area versus 1/R in the MD regime. The solid curve results from a full numerical integration (NI) of an analytic expression for m(t), obtained from Avrami's law,¹⁶ with the sinusoidal form of H(t). The dotted curve results from a numerical solution (NS) of an analytic expression obtained from a linear approximation for H(t), as for the SD regime. The transcendental equation that must be solved is analogous to Eq. (2), but contains a sum of three incomplete gamma functions.¹⁷ The MC data (solid dots), NI and NS results are in excellent agreement. For d=2 and extremely low frequencies, an asymptotic expansion of the analytic expression used to obtain the NS result gives $\langle A \rangle_{\rm MD} \propto -[\ln(H_0\omega)]^{-1}$. As in the SD case, from a log-log plot of the loop area versus frequency one can extract effective exponents from the data over nearly two decades in 1/R. However, these effective exponents depend strongly on the frequency range in which the fit is performed. Similarly, if A is plotted vs. $-[\ln(H_0\omega)]^{-1}$ as in Ref. [10], the slow crossover will result in a significant overestimate of the asymptotic exponent 1/(d-1).

A change from MD to SD behavior should appear not only as $H_0 \rightarrow H_{\text{DSP}}$, but for finite systems it should be observed when ω becomes sufficiently low that $H_{\text{s}} < H_{\text{DSP}}(L)$. The frequency of this crossover should be given by the intersection of the results for the loop areas in the SD and MD regions. The dashed curve in Fig. 3 represents the solid curve in Fig. 2, which has been rescaled so that the two results may be plotted together. The value of the loop area at the intersection is that of a loop with $H_{\text{s}} \approx H_{\text{DSP}}(L)$. While m(t) and Ado not depend on system size in the MD regime, A in the SD region, and hence the location of the crossover, depends on L.

In conclusion, we have shown that the hysteresis-loop areas for kinetic Ising ferromagnets driven by oscillating external fields vanish logarithmically with $H_0\omega$ for asymptotically low frequencies. This result should be valid for all fields and temperatures such that magnetization switching proceeds via a homogeneous nucleation-and-growth mechanism,^{10,11} in particular for both the single-droplet and multidroplet regimes considered here. For both of these regimes we stress that the asymptotic low-frequency behavior would only be seen for *extremely* low frequencies. For frequencies in a more "realistic" range we find a wide crossover, extending over many decades in frequency. Power-law fits to the loop areas over as much as four frequency decades give good agreement within the fitting range, but the resulting effective exponents depend strongly on the fitting interval. We believe our results are significant to the interpretation and comparison of results from experimental^{1,2,9} and numerical⁴⁻⁶ studies of hysteresis in ferromagnetic systems, in which power-law dependences of the loop areas have been reported with a variety of exponents.

ACKNOWLEDGMENTS

S.W.S. and P.A.R. thank P.D. Beale, G. Brown, W. Klein, M. Kolesik, and R.A. Ramos for useful discussions and the Colorado Center for Chaos and Complexity for hospitality and support during the 1997 Workshop on Nucleation Theory and Phase Transitions. Research supported in part by FSU-MARTECH, by FSU-SCRI under DOE Contract No. DE-FC05-85ER25000, and by NSF Grants No. DMR-9315969, DMR-9634873, and DMR-9520325.

REFERENCES

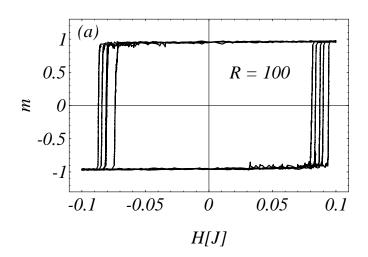
- ¹Y. He and G. Wang, Phys. Rev. Lett. **70**, 2336 (1993).
- ² J. S. Suen and J. Erskine, Phys. Rev. Lett. **78**, 3567 (1997).
- ³ M. Rao, H. Krishnamurthy, and R. Pandit, Phys. Rev. B 42, 856 (1990).
- ⁴ W. Lo and R. A. Pelcovits, Phys. Rev. A **42**, 7471 (1990).
- ⁵ S. Sengupta, Y. Marathe, and S. Puri, Phys. Rev. B **45**, 7828 (1992).
- ⁶ M. Acharyya and B. K. Chakrabarti, Phys. Rev. B **52**, 6550 (1995), and references cited therein.
- ⁷ P. Jung, G. Gray, and R. Roy, Phys. Rev. Lett. **65**, (1990).
- ⁸C. Luse and A. Zangwill, Phys. Rev. E 50, 224 (1994).
- ⁹ Q. Jiang, H.-N. Yang, and G.-C. Wang, Phys. Rev. B 52, 14911 (1995).
- ¹⁰ P. B. Thomas and D. Dhar, J. Phys. A: Math. Gen. **26**, 3973 (1993).
- ¹¹ P. D. Beale, Integrated Ferroelectrics 4, 107 (1994).
- ¹² M. Kolesik, M. A. Novotny, and P. A. Rikvold, Phys. Rev. B 56, 11791 (1997).
- ¹³ H. L. Richards, S. W. Sides, M. A. Novotny, and P. A. Rikvold, J. Magn. Magn. Mater. 150, 37 (1995); Phys. Rev. B 54, 4113 (1996); Phys. Rev. B 55, 11521 (1997).
- ¹⁴ P. A. Rikvold, H. Tomita, S. Miyashita, and S. W. Sides, Phys. Rev. E 49, 5080 (1994).
- ¹⁵S. W. Sides, R. A. Ramos, P. A. Rikvold, and M. A. Novotny, J. Appl. Phys. **79**, 6482 (1996); J. Appl. Phys. **81**, 5597 (1997).
- ¹⁶ K. Sekimoto, Physica **135A**, 328 (1986).
- ¹⁷ S. W. Sides, P. A. Rikvold, and M. A. Novotny, In preparation (1998).

FIGURES

FIG. 1. Low-frequency hysteresis loops from simulations of a kinetic Ising model. For both regimes five loops are shown, representing short portions of the entire simulation time series. (a) Loops from the single-droplet (SD) regime, using $H_0=0.1J$ at a scaled frequency of 1/R=0.01. (b) Loops from the multi-droplet (MD) regime, using $H_0=0.3J$ at a scaled frequency of 1/R=0.005.

FIG. 2. Log-log plot of $\langle A \rangle/4H_0$ vs. 1/R in the SD regime. The solid curve is obtained from the numerical solution of Eq. (2), the derivation of which is outlined in the text. The dashed line segments represent linear least-squares fits to different portions of the numerical solution data. The data that yield the effective exponent b=0.096, are centered around $\log(1/R)=-2.05$; those that yield b=0.033 are centered around $\log(1/R)=-13.38$. The two solid dots are MC simulation data. The vertical lines are not error bars; they represent the standard deviation of the loop-area distribution.

FIG. 3. Log-log plot of $\langle A \rangle/4H_0$ vs. 1/R in the MD regime. The solid curve is obtained from a full numerical integration of the time-dependent Avrami's law result for m(t), using a sinusoidal field, $H(t)=H_0 \sin \omega t$. (This calculation could not be extended to lower frequencies than those shown due to numerical difficulties.) The dotted curve is obtained from a numerical solution of an analytic expression whose derivation uses a linear approximation for the field, $H(t) \approx H_0 \omega t$. The solid dots represent MC simulations. The vertical bars denote the standard deviation in the loop-area distributions as in Fig. 2. The dashed curve represents the SD result (the solid curve in Fig. 2) after rescaling so that the SD and MD results may be compared. Figure 1 S.W. Sides MMM-Intermag 98



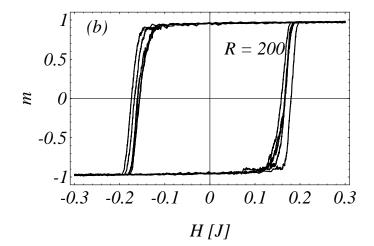
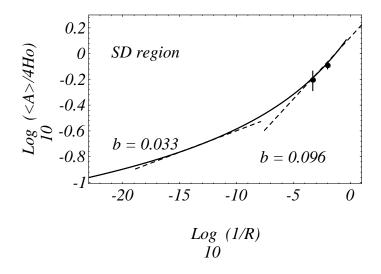
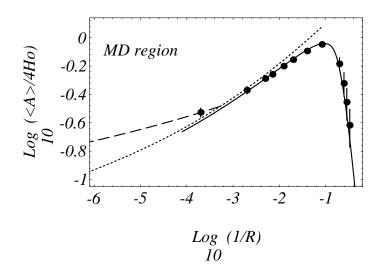


Figure 2 S.W. Sides MMM-Intermag 98



CD-06

Figure 3 S.W. Sides MMM-Intermag 98



CD-06